LOW-GRAVITY SLOSHING IN RECTANGULAR TANKS

by
Franklin T. Dodge
Luis R. Garza

TECHNICAL REPORT NO. 1
Contract NAS8-24022
Control No. DCN 1-9-75-10061 (1F), (S1)(1F)
SwRI Project 02-2578

Prepared for

National Aeronautics and Space Administration
George C. Marshall Space Flight Center
Marshall Space Flight Center, Alabama 35812

January 1970

SOUTHWEST RESEARCH INSTITUTE
SAN ANTONIO HOUSTON

CR-102800

SOUTHWEST RESEARCH INSTITUTE
Post Office Drawer 28510, 8500 Culebra Road
San Antonio, Texas 78228

LOW-GRAVITY SLOSHING IN RECTANGULAR TANKS

by
Franklin T. Dodge
Luis R. Garza

TECHNICAL REPORT NO. 1
Contract NAS8-24022
Control No. DCN 1-9-75-10061 (1F), (S1)(1F)
SwRI Project 02-2578

Prepared for

National Aeronautics and Space Administration
George C. Marshall Space Flight Center
Marshall Space Flight Center, Alabama 35812

January 1970

Approved:

H. Norman Abramson, Director
Department of Mechanical Sciences

FOREWORD

This is the seventh in a series of Technical Reports dealing with fuel sloshing under low-gravity conditions. The previous reports, all issued under Contract NAS8-20290, were: Technical Report No. 2, October 1966; Technical Report No. 4, March 1967; Technical Report No. 5, December 1967; Technical Report No. 6, February 1968; Technical Report No. 7, February 1969; and Technical Report No. 8, April 1969. A generalized digital computer program for computing the resonance parameters and equivalent mechanical model of low-gravity sloshing in an arbitrary axisymmetric tank has also been documented.

ABSTRACT

Liquid sloshing in rectangular tanks is studied theoretically and experimentally under low Bond number conditions. The static free surface shape is computed accurately by an approximate technique, and the results are used in the equations of motion for the fluid to determine the sloshing parameters; these equations are solved by Galerkin's method. The natural frequency parameter is found to increase and the equivalent slosh mass to decrease under low Bond number conditions. Nonlinearities in the experimental results prevented a close comparison of theory and test, but the trends of both are similar. Exploratory tests with square tanks show that nonlinear effects prevail also for reasonably large Bond numbers.

TABLE OF CONTENTS

LIST OF ILLUSTRATIONS

PRINCIPAL NOMENCLATURE

Nondimensional quantities are shown in parentheses at the end of the definition of the corresponding dimensional quantity

d	liquid depth
f	static free surface height ($F = f/w$)
g	gravity, or equivalent linear acceleration
h	slosh wave height ($H = h\omega/\sqrt{gw}$)
K_1	spring constant in equivalent mechanical model
K_0	nondimensional free surface curvature at $x = 0$
N_{BO}	Bond number, $\rho g w^2/\sigma$
m_1	slosh mass in equivalent mechanical model
m_T	total liquid mass per unit length of tank
u	nondimensional variable, see Equation (5a)
w	one-half tank width
x_0	amplitude of lateral excitation
X,Z	Cartesian coordinates, see Figure 1 ($X = x/w$, $Z = z/w$)
δ	nondimensional parameter, see Equation (5b)
θ	contact angle
ρ,σ	liquid density and surface tension
$\phi(x, z)$	velocity potential amplitude ($\Phi = \phi/\sqrt{gw^3}$)
ω	natural frequency ($\Omega = \omega\sqrt{2w/g}$)

I. INTRODUCTION

Certain present and contemplated space missions require that a large mass of liquid propellant remain in the tanks throughout long durations of reduced gravity flight. It has therefore become necessary to understand the dynamics of a liquid having a free surface in reduced gravity environments. As part of a continuing research program, fuel sloshing in low gravity has been analytically and experimentally investigated for cylindrical tanks with flat and inverted ellipsoidal bottoms [1,2,3], spherical tanks [3], and oblate ellipsoidal tanks [4]. Several digital computer routines also have been formulated to analyze low-gravity sloshing in axisymmetric tanks [5,6,7,8]. The utility of these researches in the national space effort is apparent.

It seems worthwhile to roundout the research by a brief study of low-gravity fuel sloshing in tanks of square and rectangular planform. Although such tanks are not used in any existing booster, it does appear likely that they will be needed in space transportation systems (STS) such as shuttle vehicles. This report presents the experimental and theoretical results of the study.

II. ANALYSIS

As is usual in theoretical fuel-sloshing research, the assumption of incompressible and inviscid fluid flow is made. The flow is further assumed to be two-dimensional; the coordinate system and symbol definitions are shown in Figure 1. The geometry of the static free surface, which is symmetrical about $x = 0$, is described by the function $f(x)$; it is a function of the surface tension σ, the density ρ, gravity g, the tank width $2w$, and the contact angle θ. The slosh wave is described by $s(x, t)$ and is determined by the fluid dynamics equations; the height of the wave above the static surface is $h(x, t) = s(x, t) - f(x)$.

Static Free Surface Shape

A force balance on an element of the free surface shows that $f(x)$ must satisfy:

$$\sigma\left\{\frac{d^2f/dx^2}{[1+(df/dx)^2]^{3/2}} - (d^2f/dx^2)_{x=0}\right\} - \rho g f = 0 \tag{1}$$

For a zero degree contact angle, the boundary conditions are

$$f = 0 \quad , \quad df/dx = 0 \quad \text{at} \quad x = 0 \tag{2}$$

$$df/dx = \infty \quad \text{at} \quad x = \pm w \tag{3}$$

Equations (1) through (3) can be solved numerically in a variety of ways but an approximate analytic integration is more appropriate here. Using the substitutions $y = df/dx$, $y\,dy/df = d^2f/dx^2$, Equation (1) can be integrated once to give

$$y^2 = \left(\frac{df}{dx}\right)^2 = \frac{1 - \left[1 - K_0(f/w) - \frac{1}{2}N_{BO}(f/w)^2\right]}{\left[1 - K_0(f/w) - \frac{1}{2}N_{BO}(f/w)^2\right]^2} \tag{4}$$

where boundary condition Equation (2) has been used to evaluate the integration constant. K_0 is the curvature (d^2f/dx^2) at the center of the tank, and $N_{BO} = \rho g w^2/\sigma$ is the Bond number. Since $df/dx = \infty$ at $x = w$, it is clear that the wave height at the wall, f_{max}, satisfies $1 - K_0(f_{max}/w) - (1/2)N_{BO}(f_{max}/w)^2 = 0$. Equation (4) can be put in a convenient nondimensional form by the substitutions

$$u^2 = K_0(f/w) + \frac{1}{2}N_{BO}(f/w)^2 \tag{5a}$$

$$\delta^2 = \frac{1}{2}K_0^2/N_{BO} \tag{5b}$$

whereupon it takes the form

$$\frac{1-u^2}{\sqrt{(2-u^2)(u^2+\delta^2)}}\frac{du}{dx} = \sqrt{\frac{N_{BO}}{2}} \tag{6}$$

The variable u runs from $u = 0$ $(f = 0)$ at $x = 0$ to $u = 1$ $(f = f_{max})$ at $x = w$. The positive square root has been taken in Equation (6) so that it is restricted to $x \leq 0$; the negative square root corresponds to $x > 0$.

Equation (6) can be integrated approximately whenever $\delta^2 \ll 1$, which will be seen to be valid whenever $N_{BO} > 6$.* Near the center of the tank $(0 \leq u^2 \leq 10\,\delta^2 \ll 1)$ u^2 is much smaller than one; thus, near the centerline, Equation (6) simplifies to:

*Equation (4) can be integrated exactly for the special case of zero gravity, $N_{BO} = 0$; the results are $f = 1 - \sqrt{1 - (x/w)^2}$ and $K_0 = 1$.

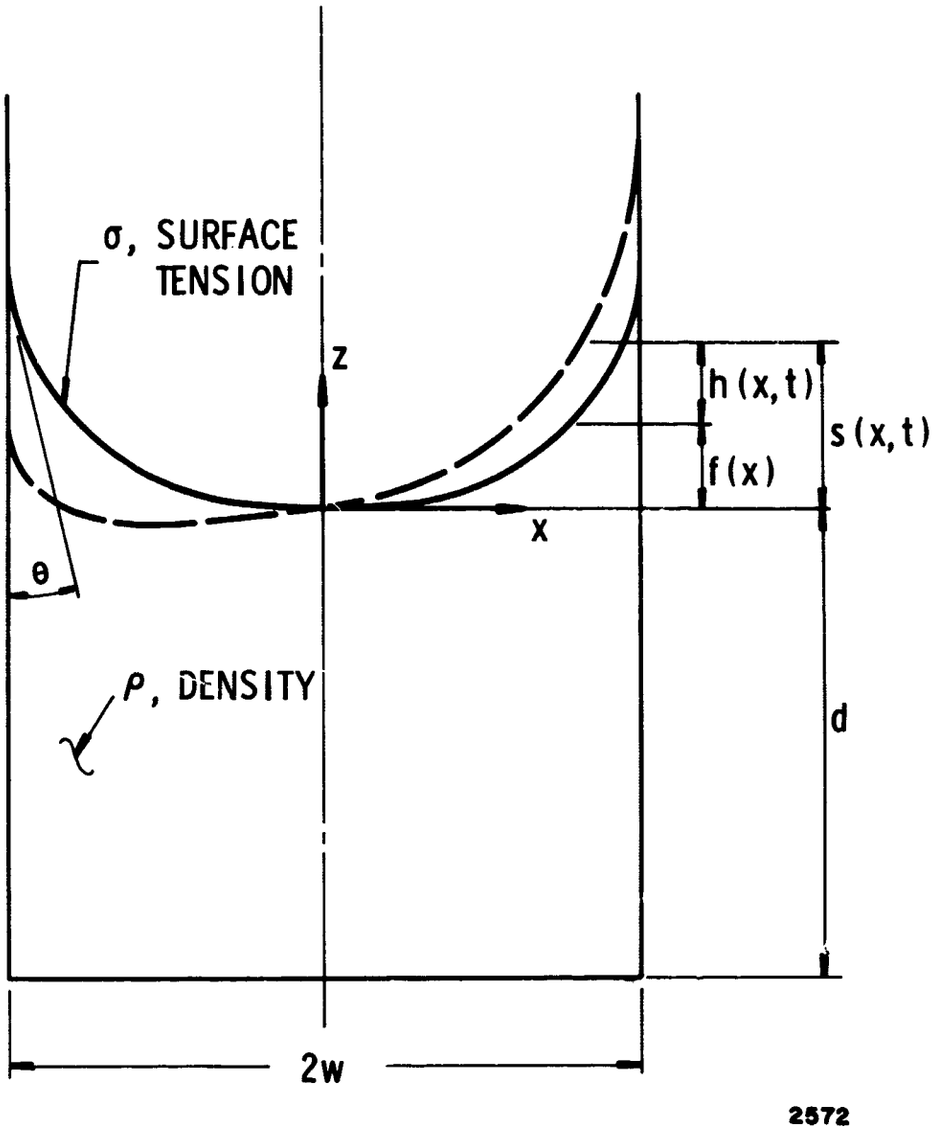

Figure 1. Coordinate System and Nomenclature

$$\frac{1}{\sqrt{\delta^2 + u^2}} \frac{du}{dx} = \sqrt{N_{BO}} \tag{7}$$

This can be integrated to give

$$ln\,[u/\delta + \sqrt{1 + (u/\delta)^2}] = x\sqrt{N_{BO}} \qquad 0 \leqslant u^2 \leqslant 10\,\delta^2 \ll 1 \tag{8}$$

after evaluating the integration constant by using $u = 0$ at $x = 0$. For the rest of the surface ($10\,\delta^2 \leqslant u^2 \leqslant 1$), Equation (6) reduces to

$$\frac{1 - u^2}{u^2\sqrt{2 - u^2}} \frac{du}{dx} = \sqrt{N_{BO}/2} \tag{9}$$

since here δ^2 is negligibly small compared to u^2. Consequently,

$$ln \frac{(1 + \sqrt{2})u}{\sqrt{2 - u^2} + \sqrt{2}} + \sqrt{2(2 - u^2)} - \sqrt{2} = (x - 1)\sqrt{N_{BO}} \qquad 10\,\delta^2 \leqslant u^2 \leqslant 1 \tag{10}$$

where the integration constant has been evaluated by using $u = 1$ at $x = 1$. Equations (8) and (1) both hold for $u^2 = 10\,\delta^2$, which thus gives an equation defining the unknown δ^2 in terms of N_{BO}:

$$ln\left[\frac{(\sqrt{10} + \sqrt{20})\,\delta}{(\sqrt{10} + \sqrt{11})(\sqrt{2 - 10\,\delta^2} + \sqrt{2})}\right] + \sqrt{2(2 - 10\,\delta^2)} - \sqrt{2} - \sqrt{N_{BO}} = 0 \tag{11}$$

The solution of Equation (11) for δ as a function of N_{BO} is shown in Figure 2, as is the resulting value of $K_0 = \delta\sqrt{2N_{BO}}$. It can be seen that $\delta^2 < 10^{-2}$ for $N_{BO} > 6$, so that $N_{BO} > 6$ can be taken as the range of validity of the proposed solutions. Curves of the static free surface shape, computed from the above equations, are shown in Figure 3 for typical values of $N_{BO} = 10, 20, 40$, and 75.

Sloshing Analysis

The characteristics of the fundamental vibration mode (sloshing mode) of the liquid are determined by a potential flow analysis. In nondimensional form, the basic equations governing the amplitudes of the wave motion, H, and the potential, Φ, are [1]:

$$\nabla^2\Phi = \frac{\partial^2\Phi}{\partial X^2} + \frac{\partial^2\Phi}{\partial Z^2} = 0 \qquad \text{everywhere in the fluid} \tag{12}$$

$$\frac{\partial\Phi}{\partial X} = 0 \quad \text{at} \quad X = \pm 1 \tag{13}$$

$$\frac{\partial\Phi}{\partial Z} = 0 \quad \text{at} \quad Z = -\frac{d}{w} \tag{14}$$

$$\frac{dH}{dX} = 0 \quad \text{at} \quad X = \pm 1 \tag{15}$$

$$H = \frac{\partial\Phi}{\partial Z} - \frac{dF}{dX}\frac{\partial\Phi}{\partial X} \quad \text{at} \quad Z = F(X) \;,\; 0 \leqslant X \leqslant 1 \tag{16}$$

$$\Omega^2\Phi - H + \frac{d}{dX}\left\{\frac{dH/dX}{N_{BO}[1 + (dF/dX)^2]^{3/2}}\right\} = 0 \quad \text{at} \quad Z = F(X) \;,\; 0 \leqslant X \leqslant 1 \tag{17}$$

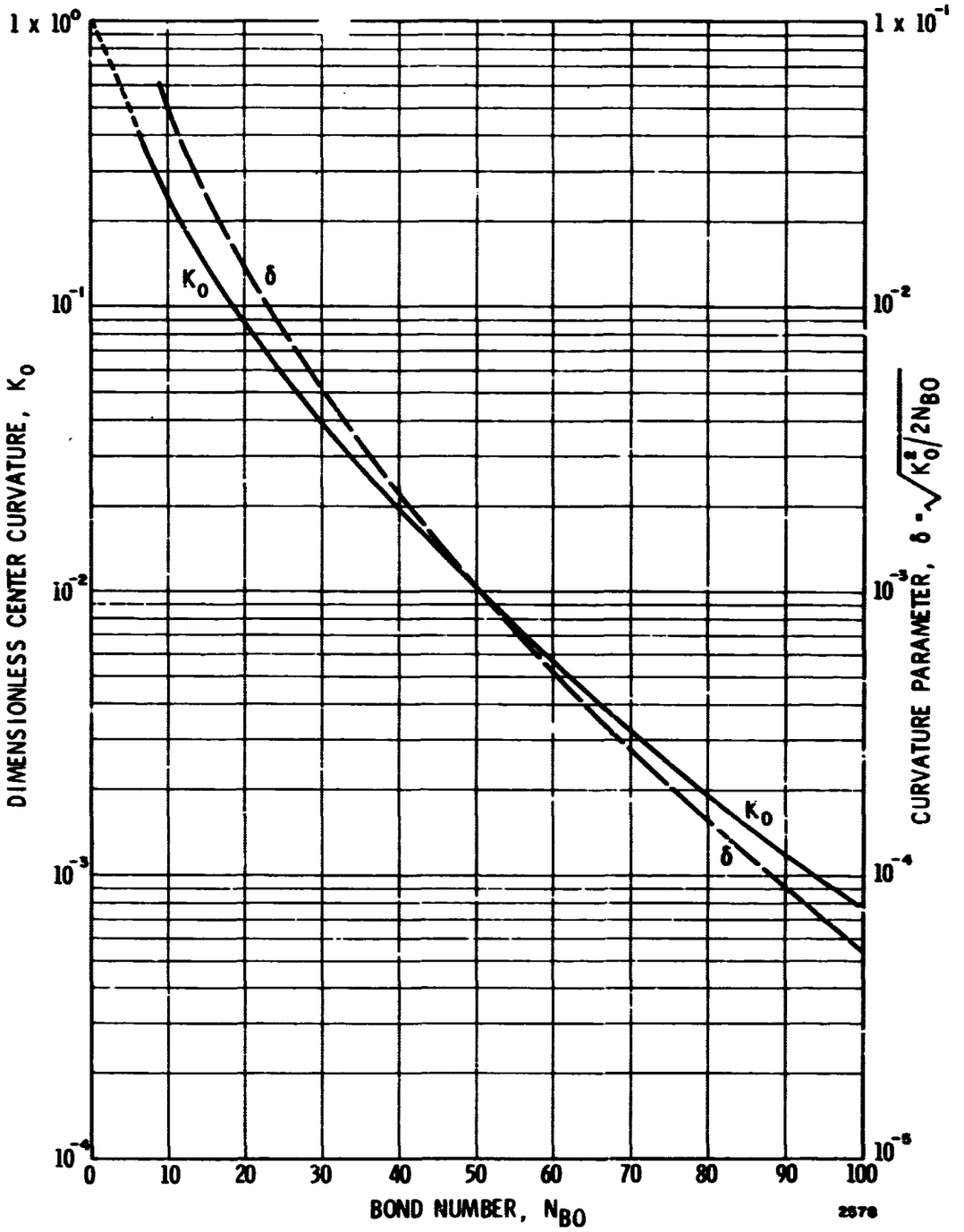

Figure 2 Stat c Free Surface Parame'ers

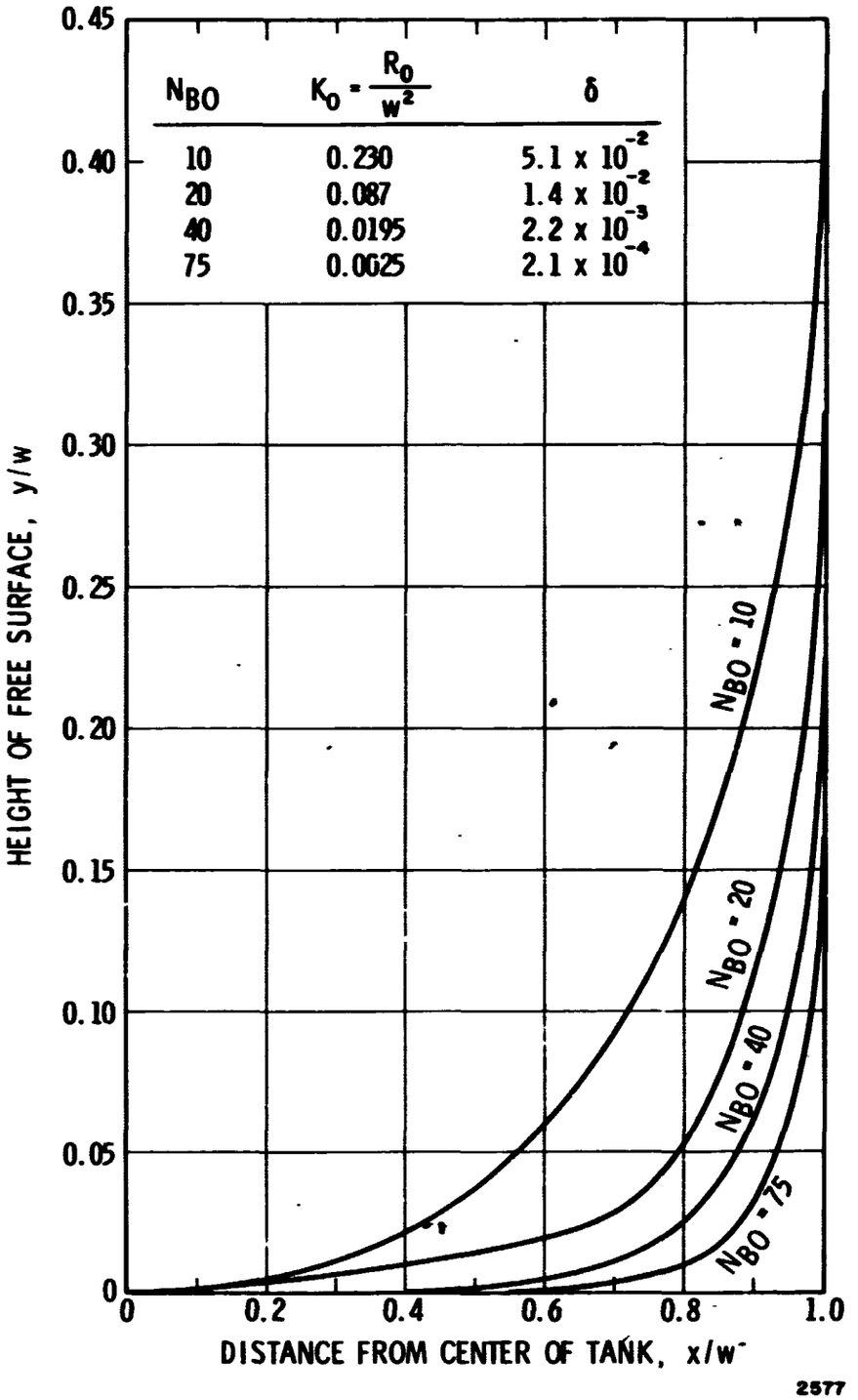

Figure 3. Shape of Free Surface for Various Bond Numbers

The nondimensional quantities are defined in the Nomenclature section. In short, the equations are the incompressibility condition, the nonpenetration of liquid through the walls and the bottom, the constancy of the contact angle,* the equivalence of the wave motion and the liquid velocity at the free surface, and Bernoulli's equation written for the free surface.

Equations (12) through (17), which do not have an "exact" analytic solution in terms of known functions, may be solved approximately by Galerkin's method. The approximating functions are taken as the normal modes for sloshing with a flat free surface ($F(X) = 0$); these are

$$\Phi(X,Z) = \sum_{n=1}^{M} a_n \Phi_n = \sum_{n=1}^{M} a_n \sin(n - 1/2)\pi X \left[\frac{\cosh \pi(n - 1/2)(Z + d/w)}{\cosh \pi(n - 1/2)(d/w)}\right] \tag{18}$$

For numerical reasons, the series is truncated after M terms and the cosh term in the denominator is used as a normalizing factor. The a_n's, thus, are the unknowns. Each Φ_n, and their sum, satisfies Equations (12), (13), and (14) identically.

The wave height, $H = \sum_{n=1}^{M} a_n H_n$, might be computed by substituting Equation (18) into Equation (16) and collecting terms; but this calculation of H does not satisfy Equation (15), at least for each H_n term by term. This is due to the assumed Φ_n's not being the true normal mode functions, term by term, of the sloshing. Presumably, if the sum $\sum_{n=1}^{M} a_n \Phi_n$ converges to the true Φ as $M \to \infty$, the sum $\sum_{n=1}^{M} a_n H_n$ also will converge to the true H and dH/dX. For numerical work, however, it is much more desirable that each H_n satisfy the correct boundary condition, Equation (15). This can be accomplished by expanding H_n, computed by substituting Equation (18) into Equation (16), into a Fourier series, thus

$$H_n = \sum_{m=1}^{\infty} b_{nm} \sin(m - 1/2)\pi X$$

$$b_{nm} = 2\int_0^1 H_n \sin(m - 1/2)\pi X \, dX \tag{19}$$

where, from Equation (16), the H_n to be inserted in the integral is

$$H_n = \pi(n - 1/2)\, a_n \left\{\sin(n - 1/2)\pi X \left[\frac{\sinh \pi(n - 1/2)(F + d/w)}{\cosh \pi(n - 1/2)(d/w)}\right] - \frac{dF}{dX} \cos(n - 1/2)\pi X \left[\frac{\cosh \pi(n - 1/2)(F + d/w)}{\cosh \pi(n - 1/2)(d/w)}\right]\right\} \tag{20}$$

Each H_n and dH_n/dX, computed using Equation (19), now satisfy the correct boundary conditions and, presumably, both converge to the true limit.

The unknown a_n's and natural frequencies Ω^2 are determined by Galerkin's method. After substituting Equations (18) and (19) into Equation (17), it becomes

$$\sum_{n=1}^{M} \left\{\Omega^2 a_n \Phi_n - a_n H_n + a_n \frac{d}{dX}\left[\frac{dH_n/dX}{N_{BO}(\sqrt{1 + (dF/dX)^2})^3}\right]\right\} = 0 \tag{21}$$

*Since $dF/dX = \infty$ at the wall for a zero-degree static contact angle, the dynamic contact angle, arccot $(dF/dX + dH/dX)$, will remain at zero for any value of dH/dX at the wall. But this is true only for $dF/dX = \infty$, so that unless $\theta = 0°$ is a singular point, it must be required that $dH/dX = 0$ at the wall for all contact angles.

Multiplying this equation by both Φ_m and a weighting factor $[1 + (dF/dX)^2]^{-1/2}$, and then integrating from 0 to 1 gives

$$\sum_{n=1}^{M} \int_0^1 \left\{ \Omega^2 a_n \Phi_n - a_n H_n + a_n \frac{d}{dX} \left[\frac{dH_n/dX}{N_{BO} (\sqrt{1 + (dF/dX)^2})^3} \right] \right\} \frac{\Phi_m \, dX}{\sqrt{1 + (dF/dX)^2}} = 0 \qquad (22)$$

This process yields a set of M linear equations:

$$\sum_{n=1}^{M} \left\{ \Omega^2 A_{mn} - B_{mn} \right\} a_n = 0 \qquad m = 1,2,3, \ldots, M \qquad (23)$$

(The weighting function is required in order that $A_{mn} = A_{nm}$ and $B_{mn} = B_{nm}$.)

The eigenvalues [2] and eigenvectors a_n may now be computed by matrix methods. The results presented here are for $M = 5$, which appears to be sufficiently large to assure convergence.

Figures 4, 5, and 6 give values of $\Omega^2 = 2\omega^2 w/g$ for various N_{BO} and depth ratios d/w. It can be seen that the natural frequency is always larger for finite N_{BO} than for the limit as $N_{BO} \to \infty$. This is a little different than the results with cylindrical tanks, for which the natural frequency in the range $N_{BO} \approx 40$ to 200 or 300 is slightly less than the infinite N_{BO} limit. (The data points on Figures 4, 5, and 6 will be discussed in the next section.)

Knowning Ω^2 and the a_n, equivalent mechanical model parameters can be computed. The x-component of the slosh force exerted on the tank by the liquid, per unit length of the wall, is

$$F_x = \iiint a_x \, dm = \rho \iint \frac{\partial V_x}{\partial t} dx \, dz = \rho \iint \frac{\partial^2 \phi}{\partial t \partial x} dx \, dz \qquad (24)$$

where a_x is the x-acceleration of the liquid and dm is the element of mass. By using nondimensional variables, and several vector identities to convert $\partial^2\phi/\partial t \partial x$ into other forms, realizing that $\nabla^2 \Phi = 0$, and using the divergence theorem, it can be seen that the force amplitude also is

$$F_x = a_1 \rho \Omega g w^2 \int_0^1 \left(\sum_{n=1}^{M} \frac{a_n}{a_1} H_n \right) dX \qquad (25)$$

where a_1 is an arbitrary amplitude and a_n/a_1 are the eigenvectors of Equation (23) for the first mode. Likewise, the amplitude of the kinetic energy is

$$KE = \frac{1}{2} a_1^2 \rho g w^3 \int_0^1 \left[\sum_{n=1}^{M} \frac{a_n}{a_1} \Phi_n \sum_{n=1}^{M} \frac{a_n}{a_1} \frac{\partial \Phi_n}{\partial X} \right]_{Z = F(X)} dX \qquad (26)$$

The corresponding quantities for a first-mode mechanical model are

$$F_x = y_0 k_1 \qquad (27)$$

$$KE = \frac{1}{2} m_1 y_0^2 \omega^2 \qquad (28)$$

where y_0 is the amplitude of vibration of the "slosh mass" m_1, and k_1 is the spring constant. Comparing Equations (27) and (28) to Equations (25) and (26) gives:

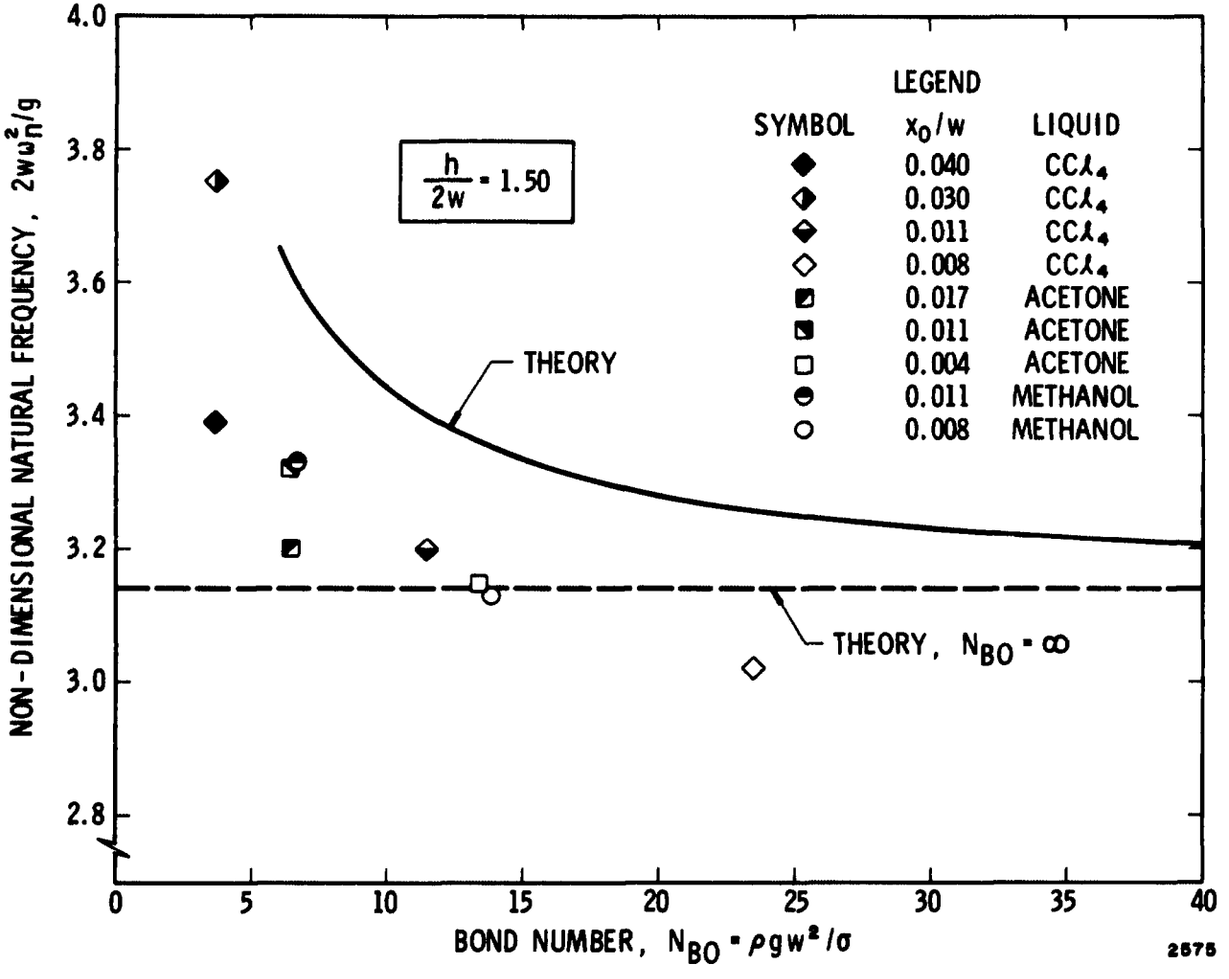

Figure 4. Natural Frequency vs N_{BO} for Depth Ratio of 1.50

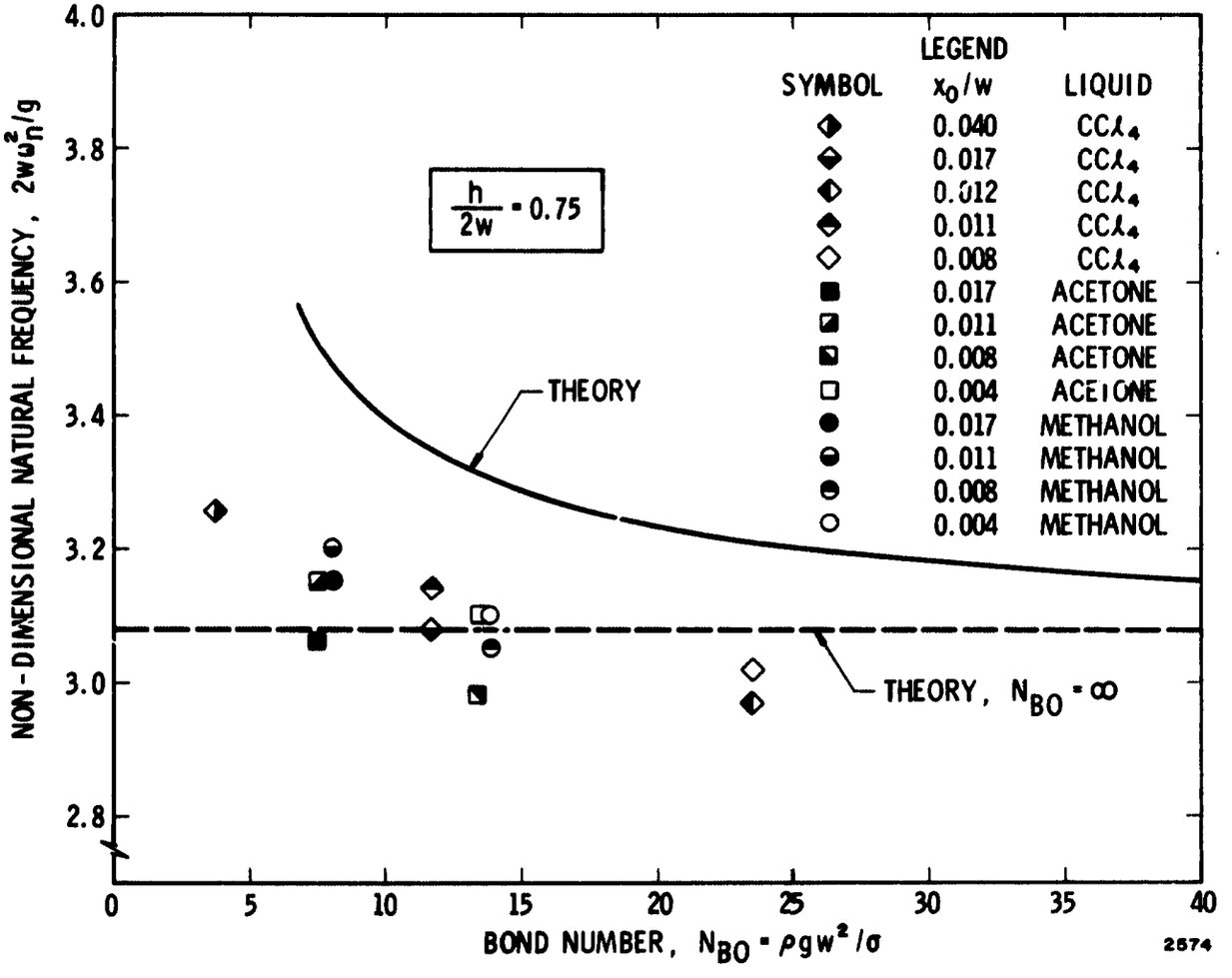

Figure 5. Natural Frequency vs N_{BO} for Depth Ratio of 0 75

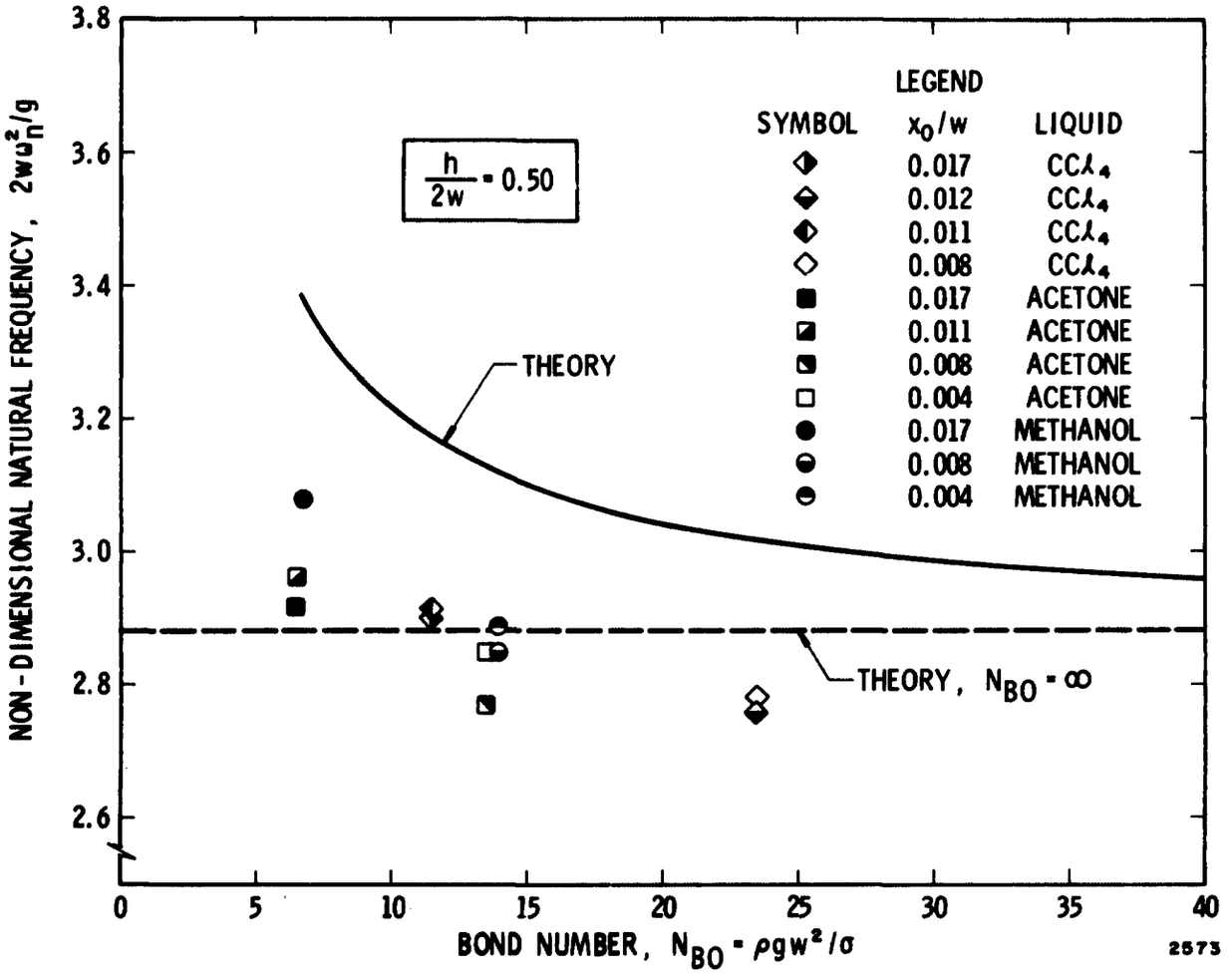

Figure 6. Natural Frequency vs N_{BO} for Depth Ratio of 0.50

$$\frac{k_1}{m_1} = \omega^2 = \Omega^2 g/w \tag{29}$$

and

$$\frac{m_1}{m_T} = \left(\frac{w}{\mathrm{d}}\right) \frac{\left[\int_0^1 \sum_{n=1}^{M} \frac{a_n}{a_1} H_n \, \mathrm{d}X\right]^2}{\int_0^1 \left[\sum_{n=1}^{M} \frac{a_n}{a_1} \Phi_n \sum_{n=1}^{M} \frac{a_n}{a_1} \frac{\partial \Phi_n}{\partial X}\right]_{Z=F(X)} \mathrm{d}X} \tag{30}$$

where $m_T = 2\rho w\,\mathrm{d}$ is the total mass of liquid in the tank per unit length. The "rigidly attached mass" is $m_0 = m_T - m_1$. The locations of m_1 and m_0 also can be computed but are not usually needed.

Figure 7 presents Equation (30) graphically for various N_{BO} and depth ratios. As can be seen, the slosh mass for finite N_{BO} is always less than it is for the limit $N_{BO} \to \infty$; this is also the case for tanks of other geometries.

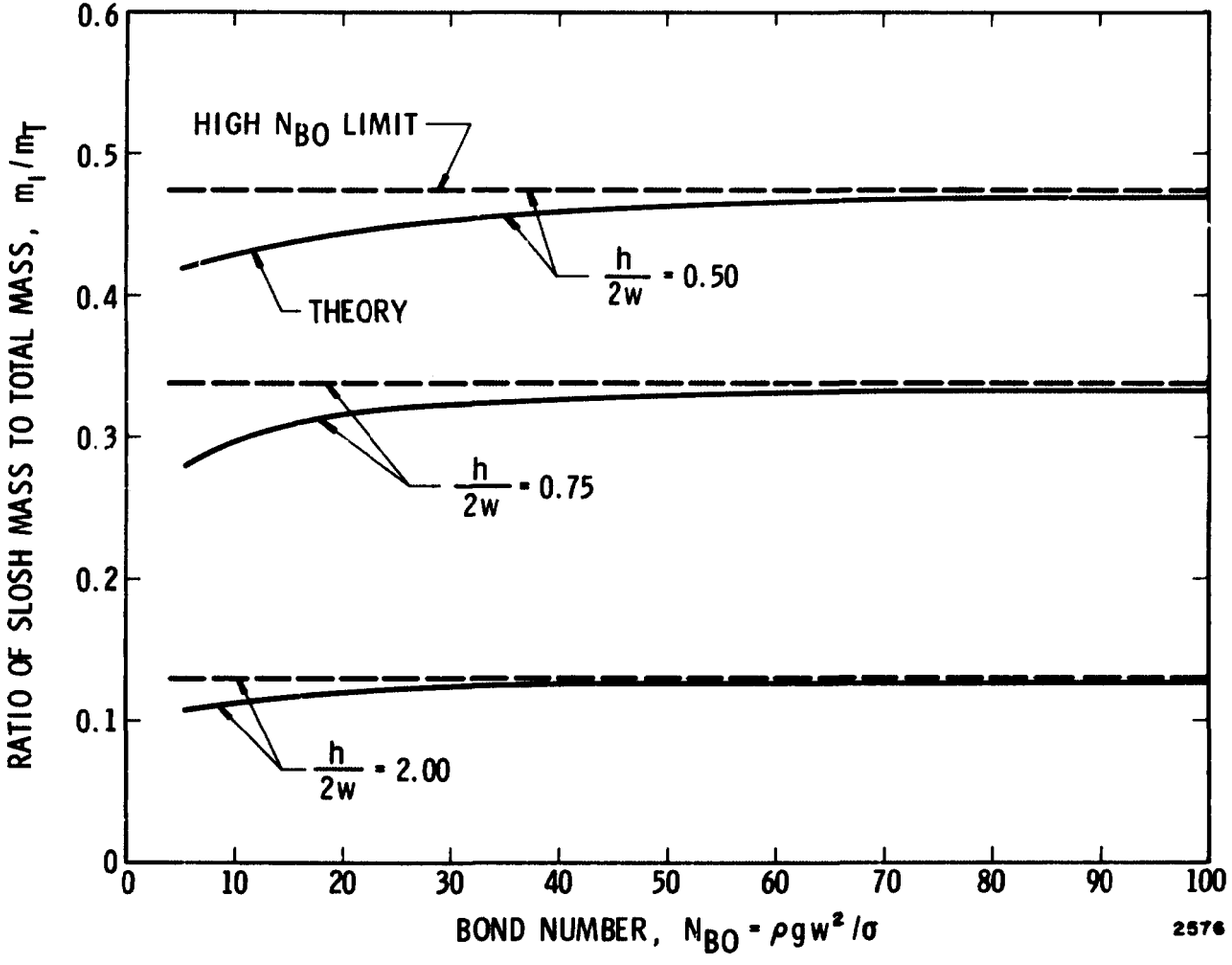

Figure 7. Variation of Slosh Mass with N_{BO} and Depth Ratio

III. EXPERIMENTAL RESULTS

All the experimental data were acquired by using small scale model tanks to obtain an appropriate Bond number similarity to large prototypes. Three different rectangular tanks were used, all having a planview width-to-length ratio small enough to insure two-dimensional flow over most of the tank; the exact planview dimensions were 0.2 X 2.0 in., 0.35 X 3.50 in., and 0.5 X 5.0 in. Three different liquids–methanol, acetone and carbon tetrachloride (CCl_4)–were used to obtain a wide range of Bond numbers with the three tanks. For comparison, a brief series of tests also were run with three different tanks of square planview, 0.35 X 0.35 in., 0.70 X 0.70 in., and 1.5 X 1.5 in.

The experimental setup, which is shown in Figure 8, is a slightly modified and improved version of the basic apparatus used previously and described in References 3 and 4; the test procedures also were similar to the previous ones. With the rectangular tank, the direction of the lateral excitation was perpendicular to the long sides; with the square tanks, the excitation was perpendicular to any two opposite sides. Enough information was taken during each test to plot the slosh force amplitude as a function of frequency around the first mode resonance; in this way, the resonant (natural) frequency, damping, and peak force could be determined.

The Bond number range covered in the rectangular tank tests was 3.75 (CCl_4 in the 0.2 X 2.0-in. tank) to 23.5 (CCl_4 in the 0.5 X 5.0-in. tank). Ratios of the liquid depth-to-width varied from 0.5 to 1.5, a depth ratio of 1.5 being effectively infinite; the liquid depth is defined as the distance from the tank bottom to the lowest point of the static free surface. (Lower Bond numbers could have been obtained by using acetone or methanol in the 0.2 X 2.0-in. tank, but the smaller densities of these two liquids would have resulted in slosh forces too small to measure accurately.)

The experimentally determined natural frequencies for the rectangular tanks are shown in Figures 4, 5, and 6. It is evident that the data points all fall below the theoretical curves, and some points even fall below the limiting frequency for $N_{BO} = \infty$. On noting the spread of the data for equal N_{BO} but different x_0, it is clear that the sloshing was decidedly nonlinear. The extent of the nonlinearity can be realized by comparing the two data points for $N_{BO} = 3.75$ in Figure 4. For $x_0/w = 0.030$, $\Omega^2 = 3.76$, which gives a natural frequency for this tank of 13.52 cps; but when $x_0/w = 0.040$, the natural frequency works out to be 12.82 cps, a change of 5.5 percent; the predicted natural frequency is 14.3 cps which is 6 percent above the highest experimentally determined frequency. The spread of the data for the higher N_{BO}'s is not quite so great, but the discrepancies between theory and test are still significant. In every case, however, the natural frequency increases as the excitation amplitude decreases. Since slosh forces smaller than 0.0001 lb cannot be measured accurately by the test apparatus, it was not possible to use very small excitation amplitudes in the hopes that nonlinear effects might have been eliminated; consequently, a direct comparison of test and theory is not possible, although the qualitative trends of both are the same.

Nonlinearities also prevent a valid comparison of the equivalent mechanical model and the tests, and likewise the damping values, which were computed on the basis of a linear response, are not accurate. Other test programs, at much higher Bond numbers, involving tank geometries possessing sharp corners also have revealed substantial nonlinearities [9,10,11]. In addition, the results of the tests with the square tanks were nonlinear, even out to Bond numbers of over 200. For example, when $N_{BO} = 210$ (CCl_4 in the 1.5 X 1.5-in. tank), Ω^2 varied from 3.05 when $x_0/w = 0.0054$ to 3.09 when $x_0/w = 0.0027$, for a depth-to-width ratio of 1.5; the theoretical value for $N_{BO} = \infty$ is 3.14. Other cases are equally nonlinear, and thus detailed results are not presented here.

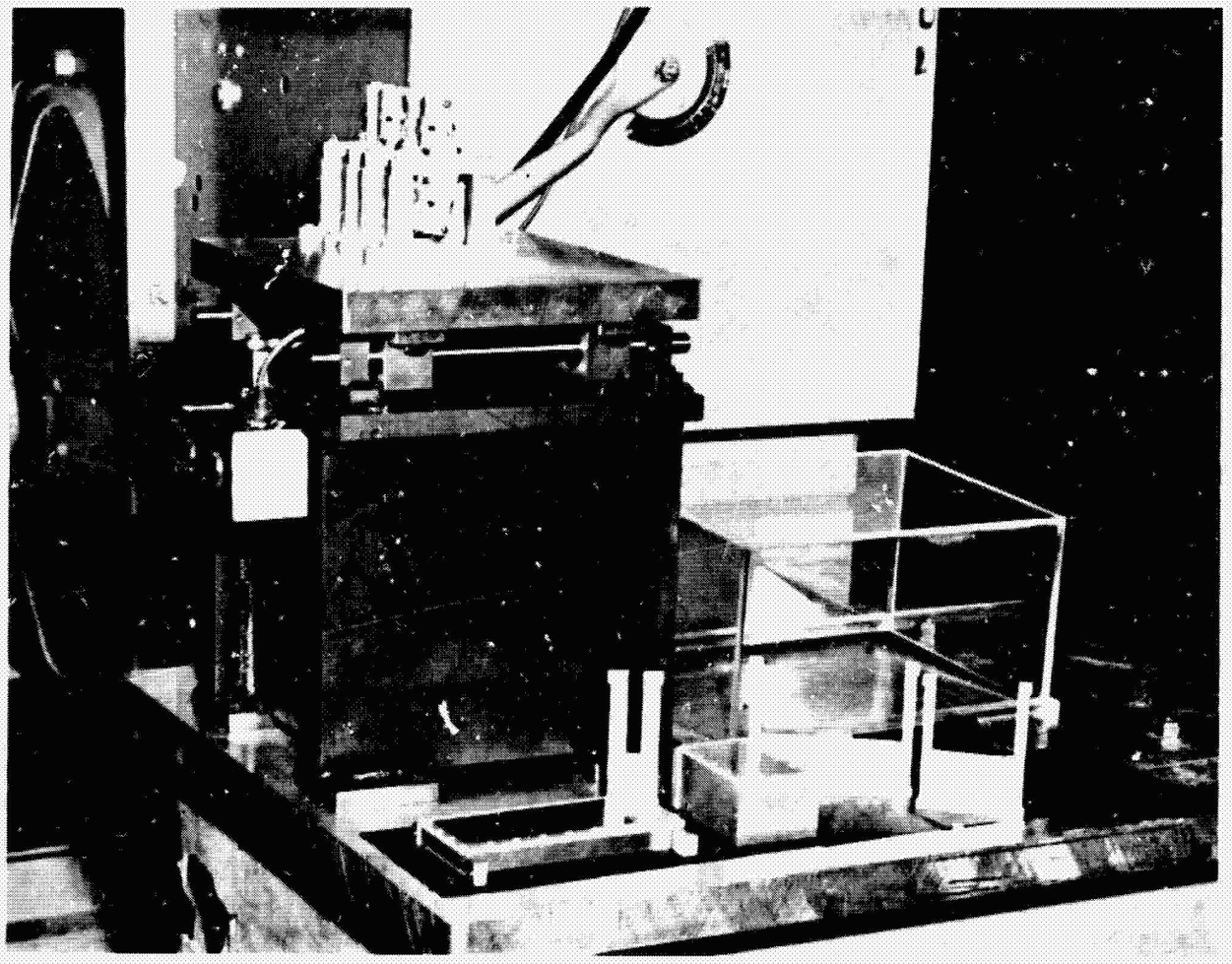

Figure 8. Experimental Apparatus

IV. CONCLUSIONS

The analytical and experimental results of this study of two-dimensional, low-gravity sloshing in rectangular tanks show, as expected, that the sloshing is qualitatively similar to that occurring for high Bond numbers (i.e., flat free surfaces). The increase in the natural frequency and the decrease in the amount of liquid participating in the sloshing in low-gravity conditions are perhaps the most interesting analytic results. The severe nonlinearities, or dependence of the slosh parameters upon amplitude, are the most significant test results. Although the trend of both test and theory is the same, the nonlinearities encountered in the tests precluded a direct comparison of the tests and the theory.

If rectangular or square tanks are to be employed in STS, the effect of the nonlinear sloshing on guidance and control should be more thoroughly explored, since a discrepancy of over 10 percent between linear theory and actual nonlinear behavior, such as was encountered in these tests, might prove to cause trouble during flight. It would be valuable to know if a "size effect" exists between these small-model tests and full-scale prototype behavior such that significant nonlinearities would not occur in large tanks, or, if, alternatively, low Bond member behavior accentuates the nonlinear behavior that always exists (even though usually negligible) regardless of the size of the tank; the present tests seem to support the latter supposition.

V. REFERENCES

1. Dodge, F.T. and Garza, L.R., "Experimental and Theoretical Studies of Liquid Sloshing at Simulated Low Gravities," *Trans. ASME, J. Applied Mechanics*, 34, No. 3, September 1967, pp 555-562. (Also, Tech. Rept. No. 2, Contract NAS8-20290, Southwest Research Institute, October 1966.)

2. Dodge, F.T. and Garza, L.R., "Simulated Low-Gravity Sloshing in Cylindrical Tanks Including Effects of Damping and Small Liquid Depth," *Proceedings of the 1968 Heat Transfer and Fluid Mechanics Institute*, pp 67-79, Stanford University Press. (Also, Tech. Rept. No. 5, Contract NAS8-20290, Southwest Research Institute, December 1967.)

3. Dodge, F.T. and Garza, L.R., "Simulated Low-Gravity Sloshing in Spherical Tanks and Cylindrical Tanks with Inverted Ellipsoidal Bottoms," Tech. Rept. No. 6, Contract NAS8-20290, Southwest Research Institute, February 1968.

4. Dodge, F.T. and Garza, L.R., "Slosh Force, Natural Frequency, and Damping of Low-Gravity Sloshing in Oblate Ellipsoidal Tanks," Tech. Rept. No. 7, Contract NAS8-20290, Southwest Research Institute, February 1969. (Also, *AIAA J. Spacecraft & Rockets*, to appear.)

5. Chu, W.H., "Low Gravity Liquid Sloshing in an Arbitrary Axisymmetric Tank Performing Translational Oscillations," Tech. Rept. No. 4, Contract NAS8-20290, Southwest Research Institute, March 1967.

6. Chu, W.H., "Low Gravity Fuel Sloshing in an Arbitrary Axisymmetric Rigid Tank," Tech. Rept. No. 8, Contract NAS8-20290, Southwest Research Institute, April 1969. (Also, *Trans. ASME, J. Applied Mechanics*, to appear.)

7. Concus, P., Crane, G.E., and Satterlee, H.M., "Small Amplitude Lateral Sloshing in a Cylindrical Tank with a Hemispherical Bottom Under Low Gravitational Conditions," NASA CR-54700, Contract NAS3-7119, Lockheed Missiles and Space Co., January 1967.

8. Concus, P., Crane, G.E., and Satterlee, H.M., "Small Amplitude Lateral Sloshing in Spheroidal Containers Under Low Gravitational Conditions," NASA CR-72500, Contract NAS3-9704, Lockheed Missiles and Space Co., February 1969.

9. Abramson, H.N., Garza, L.R., and Kana, D.D., "Some Notes on Liquid Sloshing in Compartmented Cylindrical Tanks," *ARS J.*, 32, No. 6, June 1962, pp 978-980.

10. Abramson, H.N., Chu, W.H., and Garza, L.R., "Liquid Sloshing in 45° Sector Compartmented Tanks," Tech. Rept. No. 3, Contract NAS8-1555, Southwest Research Institute, November 1962.

11. Chu, W.H., Dalzell, J.F., and Modisette, J.E., "Theoretical and Experimental Study of Ship-Roll Stabilization Tanks," *Journal of Ship Research*, 12, September 1968, pp 165-180.